SURFACE INTEGRAL EQUATION FORMULATION FOR THE ANALYSIS OF SINGLE AND MULTI-LAYER DIELECTRIC ANTENNAS

John Stevenson
University of Texas

ABSTRACT

This article studies numerically the electromagnetic scattering properties of three dimensional (3D), arbitrary shaped dielectric resonator antennas which are composed of single and multi-layered (composite) dielectric materials. Using the equivalence principle and the integral equation techniques, we first derive a surface integral equation (SIE) formulation which produces well-conditioned matrix equation. We then develop an algorithm to speed up the matrix-vector multiplications by employing the well-known method of moments (MoM) and the multilevel fast multipole method (MLFMM) on personal computer (PC) clusters. To solve the obtained integral equations, we apply a Galerkin scheme and choose the basis and testing functions as Rao-Wilton-Glisson (RWG) defined on planar patches. Finally, we present some 3D numerical examples to demonstrate the validity and accuracy of the proposed approach.

INTRODUCTION

The dielectric resonator antennas (DRAs) have received significant attention during the last two decades because of their advantages over conventional metallic antennas which suffer from problems like power loss, low bandwidth, low radiation efficiency and fabrication difficulties [1].

Figure 1 shows the configuration of a multi-layer dielectric antenna which comprises several layers of varying dielectric constant.

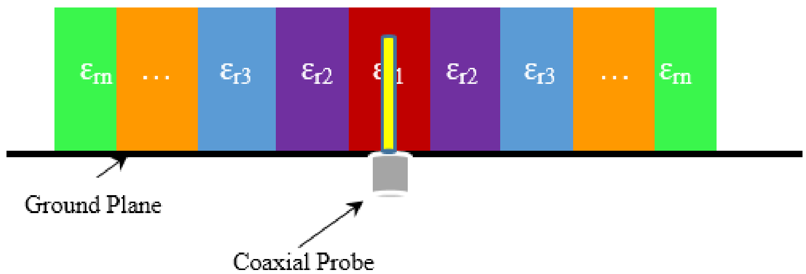

Figure 1: multi-layer dielectric resonator antenna

There is a clear need for computational and numerical analysis and design tools for calculating the performance and optimizing the parameters of dielectric antennas prior to costly prototype development. These computational methods are the building blocks of the commercial simulation software for modeling of three-dimensional metallic and dielectric antennas. One of the most general tactics to the analysis of dielectric antennas is the finite-difference time-domain (FDTD) method. The FDTD has been used by a number of authors to analyze dielectric antennas [2-5]. In [6] it is found that the FDTD is a suitable choice for axially symmetric antennas. However, in practice, the practical structures are often asymmetric such as slotted and aperture dielectric antennas. Although the FDTD is capable of modeling and analyzing an extensive range of arbitrary-shaped dielectric antennas, the complexity cost is very environment dependent and suffers from stair-casting problem [7].

The surface integral equation method is one of the most popular numerical methods in electromagnetic analysis of homogenous dielectric and composite metallic and dielectric objects. In [8] SIE based on the method of moments (MoM) has been used to simulate the interaction of light and plasmonic nanostructures. SIEs are also popular in microwave regime, and have been extensively used for the analysis of periodic lossy [9] or metallic [10] structures.

In this paper, we first derive a surface integral equation formulation to analyze electromagnetic scattering and radiation problems of all-dielectric resonator antennas. By discretizing the obtained integral equations, we acquire dense matrix equations. We then apply the well-known method of moments (MoM) along with the multilevel fast multipole method (MLFMM) to speed up vector-matrix multiplications. Proposed SIE can be extremely useful by enabling detailed analysis of novel antenna designs before their actual realizations and preventing waste of sources and time required for building and testing prototypes.

INTEGRAL EQUATION FORMULATION

Consider the case in figure 2 involving the problem of electromagnetic scattering by an arbitrary shaped, homogenous dielectric object B characterized by electrical properties (ε_i, μ_i) which is surrounded by an infinite medium having (ε_o, μ_o).

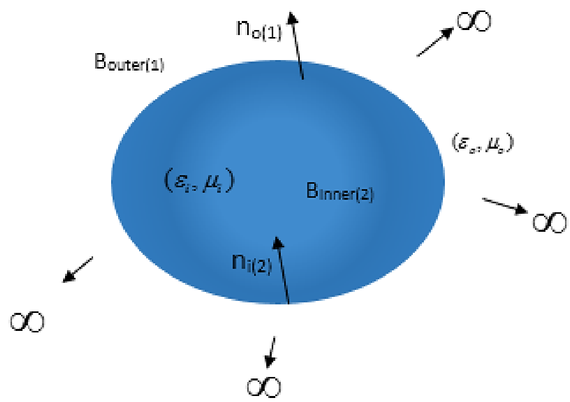

Figure 2: A homogenous region and boundary surfaces

Using the equivalence principle, the inner and outer normal (N) and tangential (T) electric and magnetic fields can be considered as:

N-EFIE(l) $$\eta_l \hat{n}_l \times \Gamma\{\mathrm{J}_l\} - \hat{n}_l \times \mathrm{K}\{\mathrm{M}_l\} = -\hat{n}_l \times \mathrm{E}_l^{inc} \qquad (1)$$

T-EFIE(l) $$\hat{n}_l \times \hat{n}_l \times \mathrm{K}\{\mathrm{M}_l\} - \eta_l \hat{n}_l \times \hat{n}_l \times \Gamma\{\mathrm{J}_l\} = (\hat{n}_l \times \hat{n}_l \times \mathrm{E}_l^{inc})_{\tan} \qquad (2)$$

N-MFIE(l) $$\hat{n}_l \times \mathrm{K}\{\mathrm{J}_l\} - \eta_l^{-1} \hat{n}_l \times \Gamma\{\mathrm{M}_l\} = -\hat{n}_l \times \mathrm{H}_l^{inc} \qquad (3)$$

T-MFIE(l) $$-\hat{n}_l \times \hat{n}_l \times \mathrm{K}\{\mathrm{J}_l\} - \eta_l^{-1} \hat{n}_l \times \hat{n}_l \times \Gamma\{\mathrm{M}_l\} = (\hat{n}_l \times \hat{n}_l \times \mathrm{H}_l^{inc})_{\tan} \qquad (4)$$

In (1)-(4), $\hat{n}_l$ denotes the inner unit normal for l=i and outer unit normal for l=o, $\eta_l = \sqrt{\mu_l / \varepsilon_l}$ is the impedance of the host medium with $l = \{i(inner), o(outer)\}$, $(\mathrm{E}_l^{inc}, \mathrm{H}_l^{inc})$ denote the incident electric and magnetic fields respectively, and $\vec{\mathrm{J}}_l$ and $\vec{\mathrm{M}}_l$ are equivalent electric and magnetic currents on the surface of the object which are related to the total electric ($\vec{E}$) and magnetic ($\vec{H}$) fields as

$$\vec{\mathrm{J}}_l(r') = \hat{n}_l \times \vec{\mathrm{H}}(r') \tag{5}$$

$$\vec{\mathrm{M}}_l(r') = \vec{\mathrm{E}}(r') \times \hat{n}_l \tag{6}$$

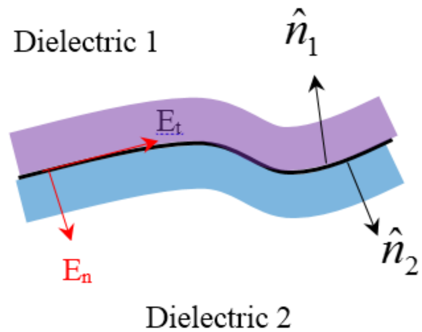

Figure 3: Boundary conditions for two dielectrics

For figure the boundary conditions can be written as

$$\mathrm{J}_1(r') = \hat{n}_1 \times \mathrm{H}_1(r') = -\mathrm{J}_2(r') = -\hat{n}_2 \times \mathrm{H}_2(r'), \tag{7}$$

$$\mathrm{M}_1(r') = \mathrm{E}(r') \times \hat{n}_1 = -\mathrm{M}_2(r') = \hat{n}_2 \times \mathrm{E}_2(r') \tag{8}$$

The operators Γ and K operators are defined as

$$\Gamma\{\vec{\mathrm{X}}\} = jk_l[\int_s \mathrm{X}(r')ds' + k_l^{-2}\int_s ds'\nabla'.\mathrm{X}(r')\nabla]\mathrm{G}_l(r,r') \tag{9}$$

$$\mathrm{K}\{\vec{\mathrm{X}}\} = \int_s \mathrm{X}(r') \times \nabla' \mathrm{G}_l(r,r')ds' \tag{10}$$

Where $k_l = \omega\sqrt{\mu_l \varepsilon_l}$ is the wavenumber and we define

$$G(\mathrm{r},\mathrm{r}') = \frac{e^{-jk_l R}}{4\pi R} \qquad (R = |r - r'|) \tag{11}$$

Which is the homogenous Green's function.

Among the various possibilities of combination of the normal and tangential electric and magnetic fields, the following mixed formulation is called the electric and magnetic current combined field integral equation (JMCFIE) [11, 12], i.e.

$$\begin{bmatrix} \sum_{l=1}^{2} \eta_l^{-1} \{\text{T-EFIE(l)}\} + \sum_{l=1}^{2} (-1)^{2l} \{\text{N-MFIE(l)}\} \\ \sum_{l=1}^{2} \eta_l \{\text{T-MFIE(l)}\} - \sum_{l=1}^{2} (-1)^{2l} \{\text{N-EFIE(l)}\} \end{bmatrix} \tag{12}$$

Using boundary conditions, it can be written as:

$$\begin{bmatrix} [Z_{11}]_{N\times N} & [Z_{12}]_{N\times N} \\ [Z_{21}]_{N\times N} & [Z_{22}]_{N\times N} \end{bmatrix} \cdot \begin{bmatrix} \mathrm{J} \\ \mathrm{M} \end{bmatrix} = \begin{bmatrix} \eta_l^{-1} (\mathrm{E}^{inc})_{\tan} - \hat{n}_l \times \mathrm{H}^{inc} \\ \eta_l (\mathrm{H}^{inc})_{\tan} + \hat{n}_l \times \mathrm{E}^{inc} \end{bmatrix} \tag{13}$$

For a composite dielectric object involving B-1 regions $B_1, B_2, \ldots, B_n$ with constitutive parameters (ε_n, μ_n) located in a host medium (ε_0, μ_0), the surface integral equation can be derived as

$$\begin{bmatrix} [\sum_{B=0}^{B-1} Z_{11,n}]_{N\times N} & [\sum_{B=0}^{B-1} Z_{12,n}]_{N\times N} \\ [\sum_{B=0}^{B-1} Z_{21,n}]_{N\times N} & [\sum_{B=0}^{B-1} Z_{22,n}]_{N\times N} \end{bmatrix} \cdot \begin{bmatrix} \mathrm{J} \\ \mathrm{M} \end{bmatrix} = \begin{bmatrix} \sum_{B=0}^{B-1} (\eta_l^{-1} (\mathrm{E}^{inc})_{\tan} - \hat{n}_l \times \mathrm{H}^{inc})_{1,n} \\ \sum_{B=0}^{B-1} (\eta_l (\mathrm{H}^{inc})_{\tan} + \hat{n}_l \times \mathrm{E}^{inc})_{2,n} \end{bmatrix} \tag{14}$$

DISCRETIZATION AND ITERATIVE SOLUTION

In order to discretize the surface integral equation in (14), one popular choice is the Rao-Wilton-Glisson (RWG) basis function [13], which discretizes the surface of the dielectric object into small elements each of which is triangle. Figure 3 depicts an RWG function on a pair of triangles.

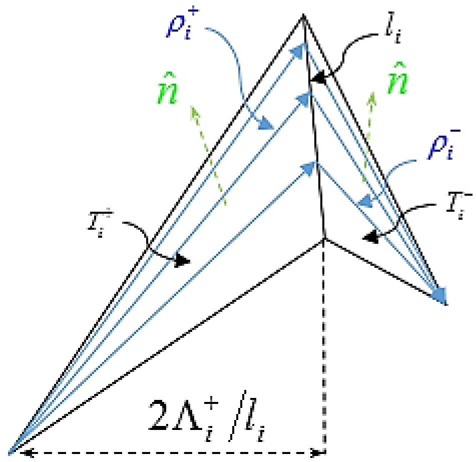

Figure 4: An RWG function

An RWG function associated with the ith edge can be defined as

$$\mathrm{f}_i(r)=\begin{cases}\dfrac{l_i\rho_i^+}{2\Lambda_i^+}, & r\in T_i^+\\ -\dfrac{l_i\rho_i^-}{2\Lambda_i^-}, & r\in T_i^-\\ 0, & otherwise\end{cases} \tag{15}$$

Where l_i is the length of the main edge, $\Lambda_i^{\pm}$ is area of triangle $T_i^{\pm}$ associated with the edge, and ρ_i^+ and ρ_i^+ are respectively position vectors with respect to the free vertex of T_i^+ and T_i^-. Also note that in figure 3, the total charge is zero for each RWG function, ensuring that all edges of T_i^+ and T_i^- are free of line charges.

Discretization of (14) using RWG functions leads to the following:

$$\begin{bmatrix}\mathrm{TT_n}+\mathrm{NK_n} & \dfrac{1}{\eta_n}\left[\mathrm{NT_n}-\mathrm{TK_n}\right]\\ \eta_n\left[\mathrm{TK_n}-\mathrm{NT_n}\right] & \mathrm{TT_n}+\mathrm{NK_n}\end{bmatrix}\cdot\begin{bmatrix}\mathrm{J}\\ \mathrm{M}\end{bmatrix}=\begin{bmatrix}\mathrm{E}_{\psi,\mathrm{n}}\\ \mathrm{H}_{\psi,\mathrm{n}}\end{bmatrix} \tag{16}$$

In which discretized operators can be simplified to the following equations after solving the interaction between the basis and testing (t_{m}) functions as

$$\underset{n}{\mathrm{T}\mathrm{T}}^{[p,q,r,s]} = \frac{\pm jk_n l_p l_q}{4\Lambda_{p,r}\Lambda_{q,s}} \int_{S_{p,r}} \rho^{+}_{p,r} dr \cdot \int_{S_{q,s}} \mathrm{G}_n(r,r')\rho^{-}_{q,s} dr' - \frac{\mp jk_n^{-1} l_p l_q}{\Lambda_{p,r}\Lambda_{q,s}} \int_{S_{p,r}} dr \cdot \int_{S_{q,s}} \mathrm{G}_n(r,r') dr' \tag{17}$$

$$\underset{n}{\mathrm{N}\mathrm{T}}^{[p,q,r,s]} = \frac{\pm jk_n l_p l_q}{4\Lambda_{p,r}\Lambda_{q,s}} \int_{S_{p,r}} \hat{n}\times\rho^{+}_{p,r} dr \cdot \int_{S_{q,s}} \mathrm{G}_n(r,r')\rho^{-}_{q,s} dr' - \frac{\mp jk_n^{-1} l_p l_q}{2\Lambda_{p,r}\Lambda_{q,s}} \int_{S_{p,r}} \hat{n}\times\rho^{+}_{p,r} dr \cdot \int_{S_{q,s}} \nabla \mathrm{G}_n(r,r') dr' \tag{18}$$

$$\underset{n}{\mathrm{N}\mathrm{K}}^{[p,q,r,s]} = \frac{\pm l_p l_q}{4\Lambda_{p,r}\Lambda_{q,s}} \int_{S_{p,r}} \hat{n}\times\rho^{+}_{p,r} dr \cdot \rho^{+}_{q,s} \times \int_{S_{q,s}} \nabla \mathrm{G}_n(r,r') dr' \tag{19}$$

$$\underset{n}{\mathrm{T}\mathrm{K}}^{[p,q,r,s]} = \frac{\pm l_p l_q}{4\Lambda_{p,r}\Lambda_{q,s}} \int_{S_{p,r}} \rho^{+}_{p,r} dr \cdot \rho^{+}_{q,s} \times \int_{S_{q,s}} \nabla \mathrm{G}_n(r,r') dr' \tag{20}$$

And

$$\mathrm{E}_{\psi,\mathrm{n}} = \pm \frac{1}{\eta_n} \int_S \mathrm{t}_{\mathrm{m}} \cdot \mathrm{E}_n^{inc}(r) dr - \int_S \mathrm{t}_{\mathrm{m}} \cdot \hat{n}\times \mathrm{H}_n^{inc}(r) dr \tag{21}$$

$$\mathrm{H}_{\psi,\mathrm{n}} = \pm \eta_n \int_S \mathrm{t}_{\mathrm{m}} \cdot \mathrm{H}_n^{inc}(r) dr + \int_S \mathrm{t}_{\mathrm{m}} \cdot \hat{n}\times \mathrm{E}_n^{inc}(r) dr \tag{22}$$

In the far-field scattering electric field can be written as:

$$\mathrm{E}^{sca} = \frac{j\omega\mu_0}{4\pi} \left[\int_S \mathrm{J}(r') e^{-jk_0\cdot r'} dr' - \eta_0^{-1} \int_S \mathrm{M}(r') e^{-jk_0\cdot r'} dr' \right] \tag{23}$$

The discretization gives:

$$\begin{aligned}
\mathrm{E}^{sca}(\theta,\phi) &= \frac{j\omega\mu_0}{4\pi}\left[\int_S \sum_{n=1}^{N} c_n^{\mathrm{J}} v_n^{\mathrm{J}}(r') e^{-jk_0\cdot r'} dr' - \eta_0^{-1}\int_S \sum_{n=1}^{N} c_n^{\mathrm{M}} v_n^{\mathrm{M}}(r') e^{-jk_0\cdot r'} dr'\right] \\
&= \pm\frac{j\omega\mu_0}{4\pi}\cdot\sum_{n=1}^{N} c_n^{\mathrm{J}} \sum_{q=1}^{2} \frac{l_n}{2\Lambda_{nq}} \int_S \rho_{n,q}^{+} e^{-jk_0\cdot r'} dr' \\
&- \frac{jk_0}{4\pi}\cdot\sum_{n=1}^{N} c_n^{\mathrm{M}} \sum_{q=1}^{2} \frac{l_n}{2\Lambda_{nq}} \int_S \rho_{n,q}^{+} e^{-jk_0\cdot r'} dr'
\end{aligned} \tag{24}$$

In which the electric (J) and magnetic (M) currents obtain from (16).

EXAMPLES

In order to show the accuracy and applicability of the proposed surface integral equation (SIE), we have considered in this section two examples of all-dielectric resonator antennas found in the literature.

The first example is the simulation of a P-shape wideband single layer dielectric antenna which is made of a dielectric material with the relative permittivity of 30 [14].

To illuminate the case we used plane wave excitation in the $\hat{k}_i$ direction with the electric field polarized in the $\hat{e}$ direction

$$\mathrm{E}^{inc}(\mathrm{r}) = \hat{e}E_0 exp(ik_0\hat{k}_i.r) \tag{25}$$

Where E_0 is the amplitude of the plane wave.

$$\mathrm{H}^{inc}(\mathrm{r}) = \frac{1}{\eta_0}\hat{k}\times\mathrm{E}^{inc}(\mathrm{r}) \tag{26}$$

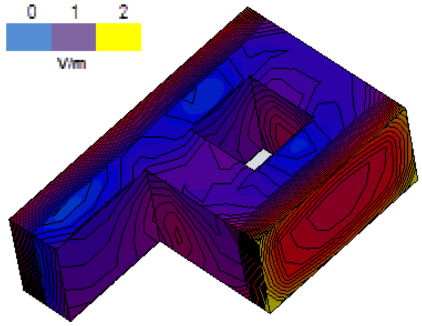

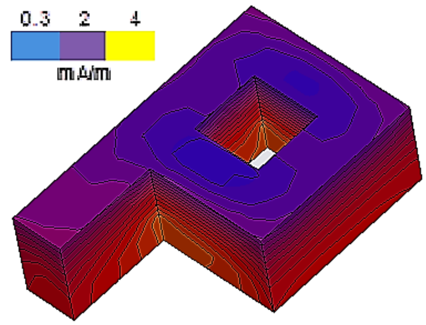

(a) Electric field distribution at 5.4GHz

(b) Magnetic field distribution at 5.4GHz

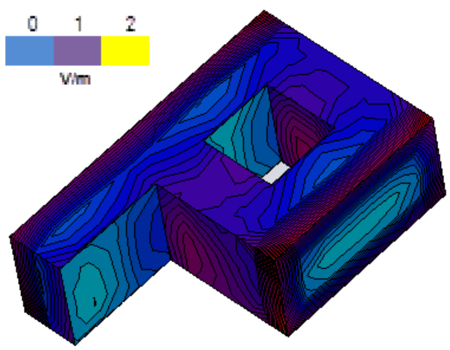

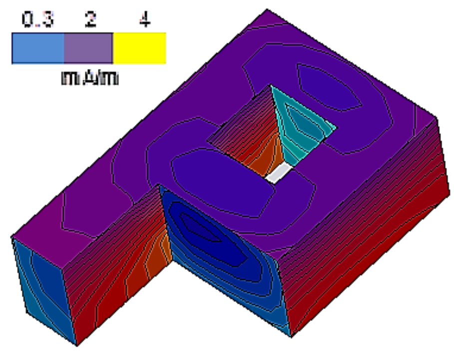

(c) Tangential electric field distribution at 5.4GHz

(d) Tangential magnetic field distribution at 5.4GHz

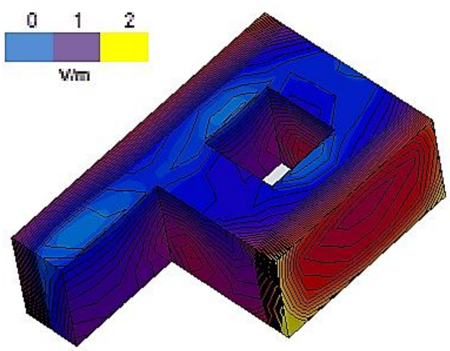

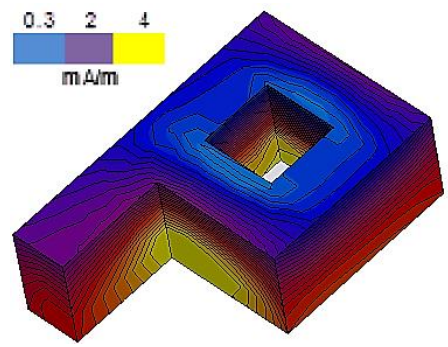

(e) Electric field distribution at 7GHz

(f) Magnetic field distribution at 7GHz

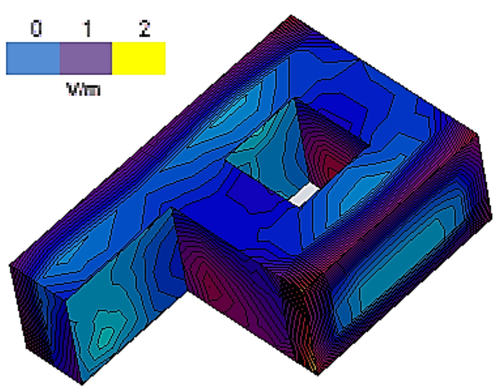

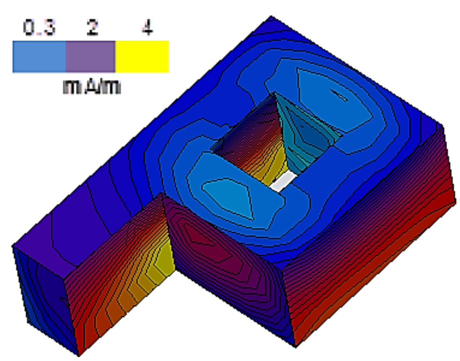

(g) Tangential electric field distribution at 7GHz

(h) Tangential magnetic field distribution at 7GHz

Figure 5: Simulation results of the P-shape dielectric antenna

Figure 5 presents the total electric field intensity (V/m) and magnetic field intensity (A/m) on the surface of the P-shape dielectric antenna when it is illuminated by a unit plane wave (1 V/m) in the +z direction.

As a second example we have considered the analysis of a concentric half-split dielectric resonator antenna (CDRA) which is developed using permittivity variation in radial direction. In this paper we have considered two CDRAs which are proposed in [15].

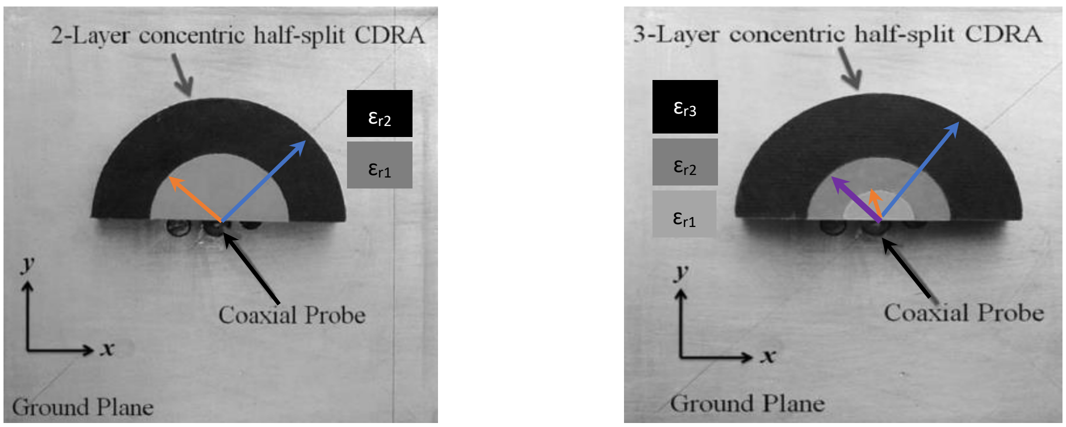

Figure 6: Fabricated two and three layer concentric dielectric antennas [15]

The fabricated two-layer and three-layer concentric composite dielectric resonator antennas are shown in figure. The dielectric constant and radius of the two-layer antenna are $\varepsilon_{r1} = 10.2, \varepsilon_{r2} = 2.32, r_1 = 11mm, r_2 = 20mm$ and $h = 11.4mm$. The optimal design parameters of the three-layer antenna are: $\varepsilon_{r1} = 10.2, \varepsilon_{r2} = 6.15, \varepsilon_{r3} = 2.32, r_1 = 5mm, r_2 = 10mm,$

$r_3 = 20mm$ and $h = 11.4mm$.

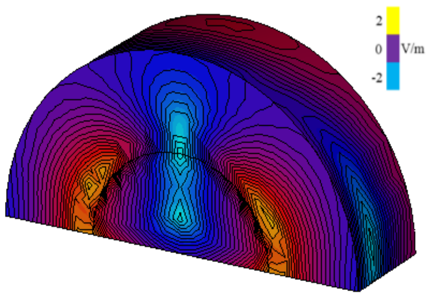

(a) Electric field distribution for two-layer DA at 6.92GHz

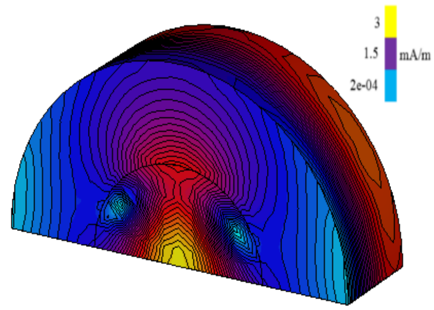

(b) Magnetic field distribution for two-layer DA at 6.92GHz

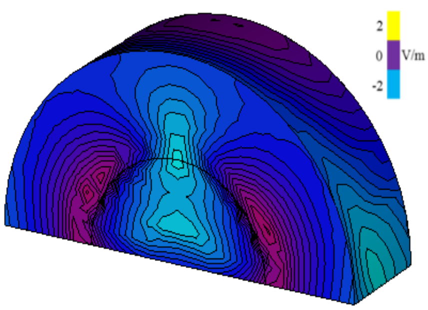

(c) Tangential electric field distribution for two-layer DA at 6.92GHz

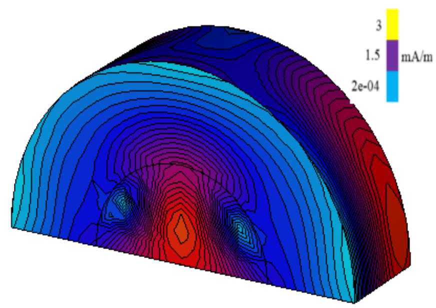

(d) Tangential magnetic field distribution for two-layer DA at 6.92GHz

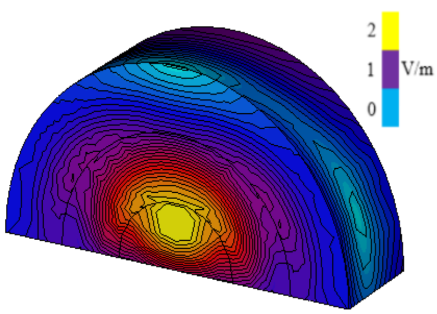

(e) Electric field distribution for three-layer DA at 5.97GHz

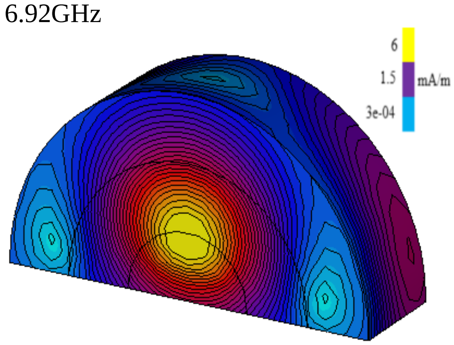

(f) Magnetic field distribution for three-layer DA at 5.97GHz

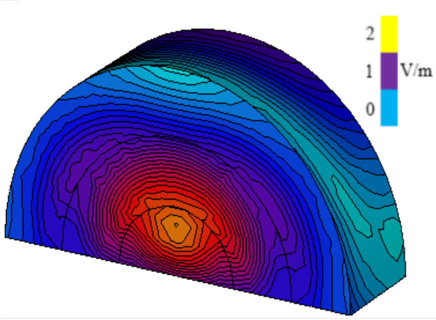

(g) Tangential electric field distribution for three-layer DA at 5.97GHz

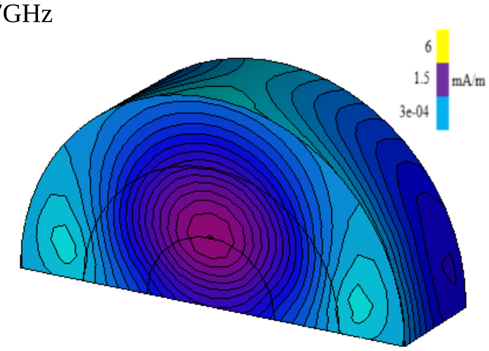

(h) Tangential magnetic field distribution for three-layer DA at 5.97GHz

Figure 7: Simulation results of the two and three-layer concentric dielectric antenna

The electric and magnetic field distribution on the surface of the proposed two and three-layer CDRA have been shown in Figure 7. The antenna is placed in the x-y direction and illuminated by a plane wave (1 V/m) in the +z direction. Computational results in figures 5 and 7 agree well with the experimental discoveries reported in the literature.

CONCLUSION

A surface integral equation formulation obtained from the Maxwell's equations has been applied to the electromagnetic scattering and radiation problems of three-dimensional (3D), arbitrary shaped single and multi-layer dielectric antennas. The obtained integral equations were discretized with the well-known method of moments (MoM), where the multilevel fast multipole method (MLFMM) has been employed to speed up matrix-vector multiplication and reduce memory requirements. Some 3D examples were presented to confirm the validity and versatility of this approach on dealing with dielectric antennas.

REFERENCES

[1] A. Kumar, V. Hamsakutty, J. Yohannan, and K. Mathew, "Microstripline fed cylindrical dielectric resonator antenna with a coplanar parasitic strip," *Progress In Electromagnetics Research,* vol. 60, pp. 143-152, 2006.

[2] S. Shum and K. Luk, "Analysis of aperture coupled rectangular dielectric resonator antenna," *Electronics Letters,* vol. 30, pp. 1726-1727, 1994.

[3] H. T. Chorsi and S. D. Gedney, "Efficient high-order analysis of bowtie nanoantennas using the locally corrected Nyström method," Opt. Exp., vol. 23, no. 24, pp. 31452–31459, Nov. 2015.

[4] E. Semouchkina, G. Semouchkin, W. Cao, and R. Mittra, "FDTD analysis of modal characteristics of dielectric resonator antennas," in *Antennas and Propagation Society International Symposium, 2002. IEEE*, 2002, pp. 466-469.

[5] H. T. Chorsi and S. D. Gedney, "Tunable plasmonic optoelectronic devices based on graphene metasurfaces," IEEE Photon. Technol. Lett., vol. 29, no. 2, pp. 228–230, Jan. 2016.

[6] N. Kaneda, B. Houshmand, and T. Itoh, "FDTD analysis of dielectric resonators with curved surfaces," *Microwave Theory and Techniques, IEEE Transactions on,* vol. 45, pp. 1645-1649, 1997.

[7] H. T. Chorsi, Y. Lee, A. Alù, and J. X. J. Zhang, "Tunable plasmonic substrates with ultrahigh Q-factor resonances," Sci. Rep. 7(1), 15985 (2017).

[8] A. M. Kern and O. J. Martin, "Surface integral formulation for 3D simulations of plasmonic and high permittivity nanostructures," *JOSA A,* vol. 26, pp. 732-740, 2009.

[9] L. C. Trintinalia and H. Ling, "Integral equation modeling of multilayered doubly-periodic lossy structures using periodic boundary condition and a connection scheme," *Antennas and Propagation, IEEE Transactions on,* vol. 52, pp. 2253-2261, 2004.

[10] H. T. Chorsi, Y. Zhu, and J. X. J. Zhang, “Patterned plasmonic surfaces—Theory, fabrication, and applications in biosensing,” J. Microelectromech. Syst., vol. 26, no. 4, pp. 718–739, Aug. 2017.

[11] P. Yla-Oijala and M. Taskinen, "Application of combined field integral equation for electromagnetic scattering by dielectric and composite objects," *Antennas and Propagation, IEEE Transactions on,* vol. 53, pp. 1168-1173, 2005.

[12] Chorsi, H.T.; Zhang, J.X.J. Apertureless near-field scanning probes based on graphene plasmonics. IEEE Photonics J. 2017, 9, 4800207.

[13] S. M. Rao, D. Wilton, and A. W. Glisson, "Electromagnetic scattering by surfaces of arbitrary shape," *Antennas and Propagation, IEEE Transactions on,* vol. 30, pp. 409-418, 1982.

[14] M. Khalily, M. K. A. Rahim, and M. R. Kamarudin, "A novel P-shape dielectric resonator antenna for wideband application," in *Applied Electromagnetics (APACE), 2010 IEEE Asia-Pacific Conference on*, 2010, pp. 1-4.

[15] R. K. Chaudhary, K. V. Srivastava, and A. Biswas, "Variation of permittivity in radial direction in concentric half-split cylindrical dielectric resonator antenna for wideband application," *International Journal of RF and Microwave Computer-Aided Engineering,* 2014.